(1969).
(5) B. F. Hoskins and B. P. Kelley, *Chem. Commun.*, 1517 (1968).
(6) P. C. Healy and A. H. White, *J. Chem. Soc., Dalton Trans.*, 1163 (1972).
(7) B. F. Hoskins and B. P. Kelley, *Chem. Commun.*, 45 (1970).
(8) P. C. Healy and E. Sinn, *Inorg. Chem.*, **14**, 109 (1975).
(9) R. J. Butcher and E. Sinn, *J. Am. Chem. Soc.*, **98**, 2440 (1976).
(10) R. J. Butcher and E. Sinn, *J. Am. Chem. Soc.*, **98**, 5159 (1976).
(11) R. J. Butcher, J. R. Ferraro, and E. Sinn, *J. Chem. Soc., Chem. Commun.*, 910 (1976).
(12) E. J. Cukauskas, B. S. Deaver, Jr., and E. Sinn, *J. Phys. Chem.*, **67**, 1257 (1977); *Inorg. Nucl. Chem. Lett.*, **13**, 283 (1977).
(13) J. G. Leipoldt and P. Coppens, *Inorg. Chem.*, **12**, 2269 (1973).
(14) E. J. Cukauskas, E. Sinn, and B. S. Deaver, Jr., *Bull. Am. Phys. Soc.*, **19**, 229, 1120 (1974).
(15) E. Sinn, *Inorg. Chem.*, **15**, 369 (1976).
(16) M. F. Tweedle and L. J. Wilson, *J. Am. Chem. Soc.*, **98**, 4824 (1976).
(17) E. V. Dose, K. M. Murphy, and L. J. Wilson, *Inorg. Chem.*, **15**, 2622 (1976).
(18) E. König and K. J. Watson, *Chem. Phys. Lett.*, **6**, 457 (1970).
(19) M. A. Hoselton, L. J. Wilson, and R. S. Drago, *J. Am. Chem. Soc.*, **97**, 1722 (1975).
(20) L. J. Wilson, D. Georges, and M. A. Hoselton, *Inorg. Chem.*, **14**, 2968 (1975).
(21) See, for example, "Inorganic Compounds with Unusual Properties", *Adv. Chem. Ser.*, **No. 150**, 128–148 (1976).
(22) See, for example, E. V. Dose, M. F. Tweedle, L. J. Wilson, and N. Sutin, *J. Am. Chem. Soc.*, **99**, 3886 (1977).
(23) (a) K. R. Kunze, D. L. Perry, and L. J. Wilson, *Inorg. Chem.*, **16**, 594 (1977); (b) E. V. Dose, M. A. Hoselton, N. Sutin, M. F. Tweedle, and L. J. Wilson, *J. Am. Chem. Soc.*, **100**, 1141 (1978).
(24) J. K. Beattie, N. Sutin, D. H. Turner, and G. W. Flynn, *J. Am. Chem. Soc.*, **95**, 2053 (1973).
(25) M. A. Hoselton, R. S. Drago, L. J. Wilson, and N. Sutin, *J. Am. Chem. Soc.*, **98**, 6967 (1976).
(26) M. G. Simmons and L. J. Wilson, *Inorg. Chem.*, **16**, 126 (1977).
(27) C. J. O'Connor, E. J. Cukauskas, B. S. Deaver, Jr., and E. Sinn, submitted for publication.
(28) P. W. R. Corfield, R. J. Doedens, and J. A. Ibers, *Inorg. Chem.*, **6**, 197 (1967).
(29) See paragraph at end of paper regarding supplementary material.
(30) D. T. Cromer and J. T. Waber, "International Tables for X-Ray Crystallography", Vol. IV, Kynoch Press, Birmingham, England, 1974.
(31) R. F. Stewart, E. R. Davidson, and W. T. Simpson, *J. Chem. Phys.*, **42**, 3175 (1965).
(32) D. T. Cromer and J. T. Waber in ref 30.
(33) D. P. Freyberg, G. M. Mockler, and E. Sinn, *J. Chem. Soc., Dalton Trans.*, 447 (1976).
(34) P. D. Cradwick, M. E. Cradwick, G. G. Dodson, D. Hall, and T. N. Waters, *Acta Crystallogr., Sect. B*, **28**, 45 (1964).
(35) A. H. Ewald, R. L. Martin, I. G. Ross, and A. H. White, *Proc. R. Soc. London, Ser. A*, **280**, 235 (1964).
(36) A. H. Ewald and E. Sinn, *Aust. J. Chem.*, **21**, 927 (1968).
(37) D. F. Lewis, S. J. Lippard, and J. A. Zubieta, *Inorg. Chem.*, **11**, 823 (1972).
(38) B. F. Hoskins and B. P. Kelley, *Chem. Commun.*, 45 (1970).
(39) See, for example, H. A. Goodwin and R. N. Sylva, *Aust. J. Chem.*, **21**, 83 (1968); C. M. Harris, T. N. Lockyer, R. L. Martin, H. R. H. Patil, E. Sinn, and I. M. Stewart, *ibid.*, **22**, 2105 (1969).
(40) B. F. Hoskins and C. D. Pannan, *Inorg. Nucl. Chem. Lett.*, **11**, 409 (1975).
(41) M. F. Tweedle, and L. J. Wilson, *Rev. Sci. Instrum.*, in press.
(42) NOTE ADDED IN PROOF. New experimental data show that the anomalously short literature bond length (2.41 Å) in FeP (Table VIII) was indeed an underestimate (A. H. White, personal communication). Our own studies confirm this and show that the true high-spin FeP complex has a longer average Fe–S bond length (2.45 Å) at ambient and at low temperatures.

Electron Density in Bis(dicarbonyl-π-cyclopentadienyliron) at Liquid Nitrogen Temperature by X-Ray and Neutron Diffraction

André Mitschler,[1a] Bernard Rees,*[1a] and Mogens S. Lehmann[1b]

Contribution from the Institut de Chimie, Université Louis Pasteur, Laboratoire de Cristallochimie et Chimie Structurale, 67070 Strasbourg-Cédex, France, and the Institut Max von Laue–Paul Langevin, 38042 Grenoble-Cédex, France.
Received September 28, 1977

Abstract: The crystal structure of the title compound has been redetermined at 74 K, both by x-ray and by neutron diffraction, and electron deformation density maps have been computed by the *X–N* method. Practically no features significantly different from zero are observed in the region of the Fe–Fe bond. The asphericity of the electron density around the iron nuclei has been related to the unequal occupancy of the 3d metal orbitals, as indicated by a semiempirical molecular orbital calculation. The molecular geometry is also discussed, with particular emphasis on the distortions of the cyclopentadienyl rings.

Introduction

In many diamagnetic binuclear complexes, a single or multiple metal–metal bond is formally required in order for each metal atom to attain the closed-shell configuration implied by their magnetic behavior. But the nature of such a bond has given rise to numerous discussions, especially when the metals are bridged by ligands. A superexchange mechanism via the bridging ligands has been invoked.[2a] A direct proof of a distinct chemical bond has been given by Coleman and Dahl,[2b] in their structure determination of $[(C_6H_5)_2PCoC_5H_5]_2$ and of $[(C_6H_5)_2PNiC_5H_5]_2$: the effect of the electron spin-coupling interaction between the metals, which exists only in the former complex, is a decrease of the metal–metal distance from 3.36 Å in the nickel complex to 2.56 Å in the cobalt complex.

The investigation, from the point of view of the distribution of electron density, of such a metal–metal bond is reported here. Bis(dicarbonyl-π-cyclopentadienyliron) [more exactly, di-μ-carbonyldicarbonyl-bis(η^5-2,4-cyclopentadien-1-yl)di-iron], $[C_5H_5Fe(CO)_2]_2$, is a diamagnetic binuclear complex, with two carbonyl bridges, for which a single Fe–Fe bond is formally required from electron bookkeeping considerations. The crystal structures of both cis and trans isomers have been reported.[3-5] We have redetermined the crystal structure of the trans isomer at low temperature both by x-ray and neutron diffraction, in order to study the charge density by the so-called *X–N* method.

Experimental Section

Air-stable crystals of *trans*-$[(\pi\text{-}C_5H_5)Fe(CO)_2]_2$ were obtained by recrystallization of commercial material in an ethyl acetate solution under argon. Relevant crystal data are given in Table I. Since the unit cell contains two molecules, in space group $P2_1/c$, the midpoint of the Fe–Fe bond is necessarily a crystallographic inversion center. No indication of a structural phase change was found during cooling to liquid nitrogen temperature. The cell constants at 74 K were determined by a least-squares refinement of the diffractometer setting

0002-7863/78/1500-3390$01.00/0

Table I. Crystal Data

trans-$[(\pi\text{-}C_5H_5)Fe(CO)_2]_2$
Space group: $P2_1/c$, $Z = 2$
Unit cell at room temperature:[4]
$a = 7.046$ (1), $b = 12.453$ (2), $c = 7.990$ (1) Å
$\beta = 108.44$ (1)°, $V = 665.1$ Å^3
Unit cell at 74 K (this work):
$a = 6.764$ (1), $b = 12.309$ (1), $c = 7.777$ (1) Å
$\beta = 106.13$ (1)°, $V = 622.0$ Å^3

Table II. X-Ray Data Collection

Crystal: spherical. Diameter: 0.25 ± 0.01 mm
Wavelength: Mo Kα λ(Kα$_1$) = 0.709 30 Å
Absorption: Linear absorption coefficient: $\mu = 22.4$ cm^{-1} ($\mu R = 0.28$). Transmission factor: 0.661–0.673.
Cryostat transmission factor = 0.920–0.931.
Recorded temperature: 74 ± 0.2 K.
Diffraction measurements:
Take-off angle: 1.2°
Monochromator: graphite
Scanning mode: continuous $\omega/2\theta$
Scanning interval in 2θ: 2.1° + $\alpha_1\alpha_2$ splitting
Scanning speed: 2°/min
Background determination: during 20 s at each end of the interval.
Distance sample–detector: 23 cm
Number of measurements (not including standard reflections):
Low-angle $2\theta < 65°$: 6711 reflections (4 equivalents)
High angle $65° < 2\theta < 110°$: 7222 reflections (2 equivalents)

angles (average for hkl and $\overline{hkl}$) of 12 x-ray reflections (Mo Kα radiation, $79° < 2\theta < 82°$).

X-Ray Data Collection. Low-temperature x-ray diffraction data were collected on a Picker diffractometer equipped with a beryllium cryostat.[6] A circulation of liquid nitrogen was ensured by pumping. Three reflections corresponding to a setting angle χ near 0, 45, and 90° were measured every 2 h to check the overall stability. No systematic variation of intensity was observed, except for a slight decrease of about 2% toward the end of data collection, for which a correction was applied. An empirical term depending on sin χ was added to the variance estimate from counting statistics, to describe the short-range fluctuations of the recorded intensity measurements. Other experimental details are listed in Table II.

Neutron Diffraction Measurements. Details are listed in Table III Neutron data were collected on the four-circle diffractometer D9 located at the hot source of the Institut Laue–Langevin high-flux beam reactor. Low temperature was obtained with an Air Products one-stage closed loop displex refrigerator.[7] To match the earlier x-ray experiment, a temperature of 74 K was chosen. As in the x-ray measurements, the spherical crystal was mounted in a general orientation in order to randomize the effect of multiple scattering. This effect has been found from measurements of extinct reflections of several crystals to be very small. The vacuum shield surrounding the crystal consists of two coaxial cylinders made of aluminum, and measurements of the beam loss in these have shown corrections to be unnecessary. The scan range was chosen so as to equalize the time spent on peak and background, and the scan ratio x in the generalized ω–$x\theta$ scan was based on experience from other crystals. The correction for background was made by use of a method which divides peak and background in such a way that $\sigma(I)/I$ is minimized.[8] (I is the integrated intensity and $\sigma(I)$ its standard deviation based on counting statistics.) Intensities were corrected for dead-time losses during the reduction of reflection profiles to squared structure amplitudes, and finally the data were corrected for second-order contamination. The size of the correction was obtained from comparison between reflections with indices hkl and $h/2k/2l/2$ where the latter are extinct. The transmission factor was measured on platelets of the material with thickness in the range 0.15–0.27 mm using a strong reflection from the sample crystal, and the resultant observed incoherent scattering cross section for hydrogen was found to be in agreement with other observations at the same wavelength.

Data Processing. After the usual Lorentz, polarization, and absorption corrections, the intensities I of crystallographically equivalent reflections were averaged and the esd's $\sigma(I)$ reduced accordingly. A term proportional to the squared intensity was added to the estimated variance of the individual intensities, so as to match in the average the sample variance calculated from the dispersion of the equivalent reflections. A large discrepancy observed at this stage for a few neutron reflections was attributed to an accidental occultation of the neutron beam during the measurement. The reflection of lowest intensity was discarded in such case. Nine additional neutron high-angle reflections (measured only once) had to be eliminated for the same reason during the least-squares refinement process; for those reflections the calculated structure factor was larger than the observed structure factor by more than ten times the standard deviation. Neutron scattering lengths, x-ray free-atom form factors (bonded-atom factor for hy-

Table III. Neutron Data Collection

Crystal	
Spherical diameter	3.90 ± 0.02 mm
Absorption	
Measured total linear absorption coefficient (average over 3 crystals)	$\mu = 1.20 \pm 0.03$ cm^{-1}
Calculated cross section for incoherent scattering of hydrogen	37×10^{-24} cm^2
Transmission factor	0.709–0.717
Recorded temperature: 74 ± 0.1 K	
Neutron beam	
Monochromator	Cu(200) in transmission geometry
Wavelength	λ = 0.748 Å
λ/2 contamination (in diffracted beam)	0.0091 (7)
Flux at sample	3×10^6 n(cm^2)$^{-1}$(s)$^{-1}$
Beam diameter at sample	8 mm
Detector gas	^{3}He
Counting chain dead-time	7×10^{-6} s
Mode of data collection	
Scanning speed	12 s/step
Data ranges: $0 < \theta < 12°$:	4 symmetry-related reflections
$12 < \theta < 22°$:	2 symmetry-related reflections
$22 < \theta < 51°$:	1006 reflections which were expected to be the strongest according to calculations.
Step scanning. Mode: ω–$x\theta$. Empirical values of x:	Number of steps per reflection:
$\theta < 22°$: $x = 1.5$	$\theta < 22°$: 51
$\theta > 22°$: $x = 1.0, 1.5, 2.0, 2.5$ for	$\theta > 22°$: 45
$\theta = 20, 30, 50, 55°$ respectively, and linear interpolation	Detector aperture diameter: 18 mm
Scan interval in θ: 1.40, 0.90, 0.90, 2.00, 4.50°	Distance sample-detector: 40 cm
for $\theta = 0, 14, 18, 31, 46°$, respectively.	Total number of reflections: 2700

Table IV. Data Processing

	X-ray full set	X-ray low angle	X-ray high angle	Neutron
Agreement between equivalent reflections: $\Sigma Av\|I - Av(I)\|/\Sigma Av(I)$	0.025	0.016	0.048	0.025
Number of reflections for least-squares input (after averaging)	5074	2266	4960	1697
Intensity requirement	$I > 3\sigma(I)$	None	None	None
$R(F) = \Sigma\|\|F_{obsd}\| - k\|F_{calcd}\|\|/\Sigma\|F_{obsd}\|$	0.030	0.024	0.093	0.016
$R_w(F^2) = [\Sigma w(\|F_{obsd}\|^2 - \|kF_{calcd}\|^2)^2/\Sigma w\|F_{obsd}\|^4]^{1/2} \simeq 2R_w(F)$	0.053	0.044	0.079	0.038
$S(F^2) = [\Sigma w(\|F_{obsd}\|^2 - \|kF_{calcd}\|^2)^2/(N_{obsd} - N_{par})]^{1/2}$	1.60	2.39	1.17	1.60
Scale factor k	3.610 (3)	3.652 (4)	3.514 (8)	4.690 (5)
Extinction parameter g ($\times 10^{-4}$)	0.13 (1)	0.19 (1)		0.165 (6)
Mosaic spread	25″	18″		20″
Largest extinction factor (reflection $11\bar{1}$)	0.84	0.79		0.73

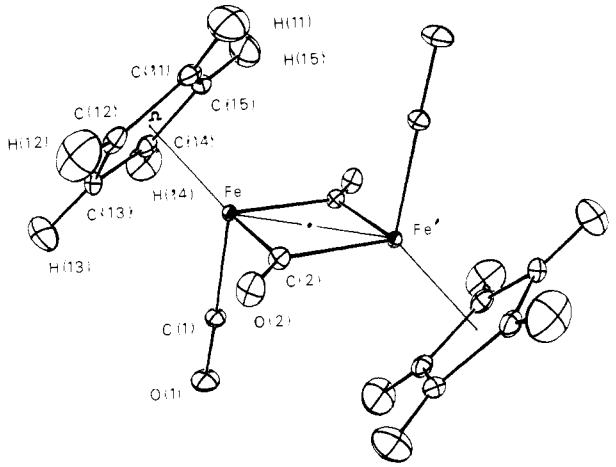

Figure 1. The bis(dicarbonyl-π-cyclopentadienyliron) molecule at 74 K. The thermal ellipsoids are for a 50% probability (from refinement of the neutron data).

drogen), and anomalous dispersion factors used in the least-squares refinements were taken from ref 9. All refinements were performed on F^2_{obsd} with weights $w = \sigma^{-2}(F^2_{obsd})$.

Secondary isotropic extinction, dominated by mosaic spread with a Lorentzian distribution function, was assumed, and the corresponding parameter g was refined, according to Becker and Coppens.[10] Results and figures of merit are given in Table IV. The good agreement factor for the neutron data is particularly noteworthy (though, of course, the low R value is partly due to the fact that the high-angle measurements were restricted to the strongest reflections; see Table III).

The positional and thermal parameters, as obtained in the least-squares refinements, are given in Table V. Three refinements are considered: (a) the conventional x-ray refinement with the full-angle data set, but imposing the usual condition $I_{obsd} > 3\sigma(I_{obsd})$; (b) a high-angle x-ray refinement ($2\theta > 65°$, i.e., $2 \sin\theta/\lambda > 1.52$ Å^{-1}) with no condition on the intensity; (c) the neutron refinement (no condition on the intensity). The neutron values of the thermal parameters were found to be systematically lower than the corresponding high-angle x-ray values. The reduction factor is not significantly anisotropic. Its value, determined by least squares (with weights depending on the estimated standard deviations), is 1.100 (7). All neutron values of the U's were then scaled by this factor. Those scaled values are in good agreement with the high-angle x-ray values, and were used in all the subsequent analyses. This systematic difference in amplitudes of thermal motion could be interpreted as indicative of an effective temperature difference of about 7 K between the two experiments. However, when high-angle and low-angle neutron data are separately refined, differences as large as 0.0030 Å^2 in the refined values of U from the two groups are obtained, whereas the positional parameters are in good agreement. The high-angle values of the thermal parameters are systematically smaller than the low-angle values, the effect being larger for U_{11} (average difference 0.0024 Å^2) than in the other directions (average 0.0009 Å^2). A possible explanation could be provided by anisotropic thermal diffuse scattering (TDS), as this is known to result in an apparent decrease of the thermal parameters, ΔU_{ij}, which varies approximately as $(\sin 2\theta)^3$.[11] A further change of the TDS contribution may result from the ω–$x\theta$ scan technique used in the measurements, since a change in x results in a change in the volume of reciprocal space swept during the scanning. The observed changes in the U's and also in the scale factor (the high-angle value is 3% smaller than the low-angle value) are comparable with those described by Helmholdt and Vos[12] for dibenzoyl, although the magnitude of the effect is somewhat larger in our case. It should be noted that, although no correlation coefficient larger than 0.5 was encountered between the U's and the scale factor in the least-squares refinements, the differences in the U's are largely reduced when the scale factor is fixed. This may be considered as an incentive to an experimental determination of the scale factor in future neutron diffraction work.

Discussion

Atomic Parameters. The x-ray and neutron positional parameters reported in Table V are never different at the 3σ level, except of course for the hydrogen atoms. On the other hand, significant differences are seen in the temperature factors, especially for those atoms for which a large anisotropy in the electron density is expected. The root mean square amplitude of motion along the principal axes resulting from the three refinements is given in Table VI for the carbonyl atoms. The neutron values have been scaled as described above. The direction of smallest amplitude (axis 1 in the table) is that of the bond axis. It is seen that the conventional x-ray refinement results in a larger amplitude in this direction, owing to the concentration of electron density along the bond axis (see below). The high-angle x-ray refinement yields values much closer to the neutron values, but in most cases intermediate between the conventional x-ray and the neutron results, which seems to indicate that some small error due to bonding effects still affects even the high-angle x-ray temperature factors.

Molecular Geometry. The molecule, with thermal ellipsoids at the 50% probability level, is shown in Figure 1. Bond lengths and angles are reported in Table VII. The good agreement between neutron and x-ray results (except for hydrogen) is again noticeable. The discussion which follows is based only on the neutron results.

Bond length corrections for thermal vibration in the cyclopentadienyl ring are based on a thermal motion analysis,[13] which showed that the five carbon atoms behave rigidly within the limits of experimental accuracy, whereas the hydrogen atoms undergo additional riding motion. Although the rest of the molecule is not rigid, the rigid-body approximation (excluding the hydrogen atoms from the calculation) was used to correct the Fe–Fe, Fe–C, and C–O bond lengths.

The centroids Ω and Ω' of the cyclopentadienyls, the two iron atoms, and the terminal carbonyls C(1) O(1) and C′(1) O′(1) are very nearly coplanar (within 0.02 Å), and their mean plane is perpendicular (the angle is 90.3°) to the mean plane of the cyclopentadienyl, but makes an angle of 14.3° with direction

Table V. Relative Coordinates ($\times 10^5$) and Thermal Motion Parameters ($\times 10^4$ Å^2)[e]

		x	y	z	U_{11}	U_{22}	U_{33}	U_{12}	U_{13}	U_{23}
Fe	*a*	8759 (2)	5866 (1)	13 372 (1)	71.9 (3)	73.6 (4)	67.4 (3)	3.8 (4)	6.9 (2)	−6.3 (4)
	b	8756 (2)	5867 (1)	13 374 (2)	67.3 (4)	69.6 (6)	63.0 (4)	2.5 (5)	5.9 (2)	−5.0 (4)
	c	8765 (5)	5866 (3)	13 372 (4)	59.9 (10)	59.1 (10)	55.0 (10)	2.7 (11)	4.9 (8)	−6.2 (11)
	d				66.5 (12)	65.5 (12)	61.1 (12)	3.0 (12)	5.4 (9)	−6.9 (12)
O(1)	*a*	−22 566 (12)	22 765 (6)	6741 (11)	186 (3)	168 (3)	259 (4)	76 (2)	10 (3)	−35 (3)
	b	−22 603 (23)	22 773 (14)	6766 (22)	177 (4)	146 (5)	265 (4)	88 (3)	10 (3)	−26 (4)
	c	−22 559 (10)	22 775 (6)	6758 (9)	163 (3)	137 (3)	245 (3)	84 (2)	12 (3)	−22 (2)
	d				181 (3)	152 (3)	274 (4)	93 (3)	14 (3)	−24 (3)
O(2)	*a*	18 740 (10)	10 962 (5)	−19 841 (9)	161 (3)	175 (3)	129 (2)	−42 (3)	53 (2)	23 (2)
	b	18 746 (18)	10 950 (11)	−19 853 (13)	162 (3)	168 (4)	124 (2)	−45 (3)	57 (2)	26 (2)
	c	18 737 (10)	10 958 (5)	−19 823 (8)	150 (3)	155 (3)	107 (2)	−51 (2)	51 (2)	24 (2)
	d				166 (3)	172 (3)	119 (2)	−56 (2)	56 (2)	26 (2)
C(1)	*a*	−10 351 (13)	16 007 (7)	9174 (11)	118 (3)	120 (3)	131 (3)	11 (2)	10 (2)	−20 (2)
	b	−10 367 (18)	16 020 (11)	9153 (15)	108 (3)	103 (4)	136 (3)	25 (3)	10 (2)	−18 (2)
	c	−10 338 (8)	16 030 (4)	9153 (7)	101 (2)	85 (2)	127 (2)	24 (2)	8 (2)	−17 (2)
	d				112 (2)	94 (2)	141 (2)	27 (2)	9 (2)	−19 (2)
C(2)	*a*	10 352 (12)	5950 (6)	−10 997 (10)	100 (2)	106 (3)	94 (2)	3 (3)	20 (2)	5 (2)
	b	10 358 (14)	5940 (13)	−11 013 (10)	96 (2)	101 (3)	89 (2)	−8 (3)	24 (2)	11 (3)
	c	10 356 (7)	5951 (4)	−11 000 (6)	85 (2)	92 (2)	80 (2)	8 (2)	25 (1)	11 (2)
	d				94 (2)	102 (2)	89 (2)	−9 (2)	27 (1)	12 (2)
C(11)	*a*	34 353 (14)	−3480 (7)	28 469 (12)	125 (3)	125 (3)	140 (3)	23 (2)	−22 (3)	−5 (2)
	b	34 321 (21)	−3530 (13)	28 502 (17)	123 (3)	113 (4)	136 (3)	24 (3)	−15 (3)	−3 (2)
	c	34 365 (8)	−3499 (4)	28 469 (7)	110 (2)	95 (2)	128 (2)	19 (2)	−19 (2)	−5 (2)
	d				122 (2)	106 (2)	142 (2)	21 (2)	−21 (2)	−6 (2)
C(12)	*a*	22 965 (14	426 (8)	40 022 (11)	134 (3)	203 (4)	96 (3)	−21 (3)	−5 (2)	34 (3)
	b	22 946 (21)	456 (14)	40 024 (15)	133 (3)	179 (6)	93 (6)	−21 (3)	−4 (2)	31 (3)
	c	22 939 (8)	424 (5)	40 033 (7)	121 (2)	166 (2)	85 (2)	−15 (2)	−1 (2)	29 (2)
	d				134 (3)	185 (3)	94 (2)	−17 (2)	−1 (2)	32 (2)
C(13)	*a*	22 833 (14)	11 906 (7)	39 145 (11)	133 (3)	193 (4)	93 (3)	10 (3)	5 (2)	−45 (2)
	b	22 805 (21)	11 933 (13)	39 156 (15)	129 (3)	176 (5)	95 (3)	9 (3)	8 (2)	−44 (3)
	c	22 837 (8)	11 919 (5)	39 169 (7)	120 (2)	157 (2)	86 (2)	12 (2)	9 (2)	−43 (2)
	d				134 (2)	174 (3)	95 (2)	13 (2)	10 (2)	−47 (2)
C(14)	*a*	34 591 (13)	15 157 (7)	27 276 (11)	121 (3)	124 (3)	133 (3)	−21 (2)	−8 (2)	−14 (2)
	b	34 651 (20)	15 158 (13)	27 243 (16)	120 (3)	111 (4)	132 (3)	−17 (3)	−3 (3)	−15 (3)
	c	34 603 (8)	15 164 (4)	27 264 (7)	107 (2)	95 (2)	121 (2)	−20 (2)	−1 (2)	−14 (2)
	d				119 (2)	106 (2)	135 (2)	−23 (2)	−1 (2)	−16 (2)
C(15)	*a*	41 756 (12)	5616 (7)	20 875 (11)	87 (2)	189 (3)	120 (3)	8 (3)	12 (2)	−15 (3)
	b	41 745 (14)	5602 (15)	20 855 (13)	88 (2)	160 (4)	121 (2)	3 (3)	17 (2)	−18 (3)
	c	41 775 (7)	5642 (5)	20 878 (6)	79 (2)	149 (2)	107 (2)	4 (2)	16 (2)	−17 (2)
	d				86 (2)	166 (2)	118 (2)	5 (2)	18 (2)	−19 (2)
H(11)	*a*	36 523 (229)	−11 112 (113)	26 262 (207)	250 (36)					
	c	37 159 (22)	−11 939 (10)	26 147 (19)	366 (7)	162 (5)	398 (7)	74 (5)	12 (6)	−35 (5)
	d				406 (8)	180 (6)	441 (8)	82 (6)	13 (7)	−39 (6)
H(12)	*a*	16 565 (250)	−4018 (109)	46 950 (211)	246 (38)					
	c	15 357 (23)	−4479 (13)	47 781 (18)	339 (7)	441 (8)	272 (6)	−86 (6)	96 (6)	139 (6)
	d				377 (8)	489 (9)	302 (7)	−95 (7)	107 (6)	154 (6)
H(13)	*a*	15 706 (226)	16 787 (114)	45 302 (189)	260 (37)					
	c	15 357 (22)	17 292 (12)	46 363 (18)	319 (7)	403 (8)	278 (6)	73 (6)	97 (6)	−153 (6)
	d				354 (8)	447 (9)	308 (7)	82 (7)	107 (6)	−170 (6)
H(14)	*a*	36 818 (216)	22 821 (101)	24 173 (191)	186 (34)					
	c	37 306 (23)	23 443 (10)	23 949 (19)	355 (7)	173 (5)	376 (7)	−70 (5)	34 (6)	37 (5)
	d				394 (8)	192 (6)	418 (8)	−78 (6)	37 (6)	41 (6)
H(15)	*a*	50 477 (238)	5323 (92)	12 601 (200)	172 (35)					
	c	51 001 (20)	5322 (12)	11 537 (17)	235 (6)	457 (8)	283 (6)	4 (6)	148 (5)	−44 (6)
	d				261 (6)	507 (9)	314 (7)	4 (6)	165 (6)	−49 (6)

[a] From conventional refinement of the full set of x-ray data, with the condition $I_{obsd} > 3\sigma(I_{obsd})$. An isotropic thermal motion is assumed for the hydrogen atoms. [b] From refinement of the high-angle x-ray data ($2 \sin \theta/\lambda > 1.52$ Å^{-1}). No condition on observed intensity. [c] From refinement of the neutron data. No condition on observed intensity. [d] As *c*, *U* values scaled (see text). [e] The temperature factor is $\exp(-2\pi^2 \cdot \Sigma_i \Sigma_j U_{ij} h_i a_i^* h_j a_j^*)$. Esd's are given in brackets for the rightmost significant digits.

ΩC(11). This angle is only 4.9° at room temperature.[4] This abrupt change contrasts with the generally good agreement of bond lengths (after corrections for thermal motion), and is obviously related to the very small rotational barrier of the cyclopentadienyl.[14] Figure 2 shows that the plane Fe Ω C(11) is an approximate mirror plane of the cyclopentadienyl ring, which is significantly distorted: the C–C lengths range from 1.416 to 1.441 Å, in contrast with the C–H lengths, which are remarkably constant (1.105–1.107 Å). This distortion in the bond lengths will be discussed below. The whole ring is not planar but slightly bent around an axis perpendicular to the "mirror" plane. This may be compared to ferrocene[14] and to benzene–metal complexes,[15] where an umbrella structure is observed, the carbon atoms remaining coplanar.

It is interesting to compare the geometry of bis(dicarbonyl-π-cyclopentadienyliron) to that of the parent but more symmetric complexes ferrocene[14] and nonacarbonyldiiron.[16] The Fe–C distances to the cyclopentadienyl ring are consistently longer by 0.05–0.09 Å than in ferrocene (2.058 Å),[14] whereas the Fe–C(O) distances are shortened by 0.08 Å when

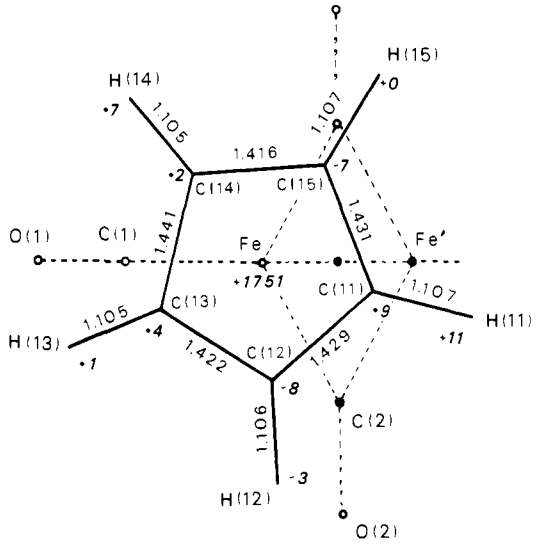

Figure 2. Projection on the cyclopentadienyl plane. Neutron results. The bond lengths (Å) are corrected for thermal libration. The distance of each nucleus from the least-squares plane is given in 10^{-3} Å units; the corresponding σ is about 0.5×10^{-3} Å for carbon and 1.2×10^{-3} Å for hydrogen atoms.

Table VI. Root Mean Square Amplitudes of Motion along the Principal Axes in the Carbonyl Groups (Unit: 10^{-3} Å): (a) Conventional X-Ray Refinement; (b) High-Angle X-Ray Refinement; (c) Neutron Refinement (Scaled U's).[a]

	Axis 1	Axis 2	Axis 3
O(1) (a)	99	141	186
(b)	84	143	185
(c)	85	147	187
O(2) (a)	96	123	147
(b)	89	123	147
(c)	84	121	152
C(1) (a)	102	104	131
(b)	89	103	132
(c)	86	104	135
C(2) (a)	94	103	104
(b)	90	96	107
(c)	87	97	107

[a] The conventional x-ray refinement is seen to result in a consistent apparent reduction of the anisotropy of the thermal motion.

compared to $Fe_2(CO)_9$.[16] This indicated that, when both ligands C_5H_5 and CO are in competition, the former is more weakly and the latter more strongly bonded. A corresponding expected lengthening of the CO bonds is not observed, both the terminal and the bridged carbonyl bond lengths being the same, within 0.004 Å, as in $Fe_2(CO)_9$, although the riding model (O on C) used for correction of thermal motion effects in $Fe_2(CO)_9$ could have resulted in an overcorrection. On the other hand, the average C-C length, 1.428 Å, is in good agreement with the one obtained by electron diffraction in ferrocene (1.431 ± 0.005 Å).[14]

Electron Density

The deformation density $\Delta\rho = \rho_{crystal} - \Sigma\rho_{free\ atoms}$ has been computed by Fourier transformation of $F_{obsd,\ x\text{-}ray}/k - F_{calcd}$, with a cutoff value $2 \sin\theta_{max}/\lambda = 1.52$ Å^{-1}. The factors F_{calcd} were calculated with the form factors of the spherical atoms in their ground state,[9] with the distribution of the nuclei as determined from the neutron refinement (thermal parameters scaled, see above). The factors $F_{obsd,\ x\text{-}ray}$ were corrected for anomalous dispersion effects. Their sign was assumed to be that of F_{calcd}. The scale factor k was determined by a least-squares refinement in which positional and thermal parameters were fixed at their neutron values. Sections of the deformation density are shown in Figures 3-5. Figure 6 shows the estimated standard deviation $\sigma(\Delta\rho)$ along three bond directions.[17] A value $\sigma(k)/k = 0.002$ was assumed as the probable error arising from the procedure used in the determination of k. This value results from test calculations performed for the complex $Cr(CO)_6$.[17]

All peaks corresponding to electron accumulation in the C-C, C-H, C-O bonds and in the regions of the carbonyl carbon and oxygen lone pairs are visible in the deformation density maps. This contrasts with the Fe-Fe bond: the residues between the bonded iron atoms are small and generally insignificant, except at a short distance from the metal nucleus. There is some analogy with acetylenebis(cyclopentadienylnickel),[18] where a double maximum was found between the nickel atoms, with a deformation density close to zero at the midpoint. In the iron atom region, the density is practically centrosymmetric around the metal nucleus. The density in this region shows some features analogous to what is observed in an octahedral complex like $Cr(CO)_6$,[19] namely, a concentration in directions corresponding to the threefold axes of the octahedron (one of those axes becomes here the direction Fe-Ω) and an electron deficiency in the direction of the carbonyls. But at the same time, there is a tendency toward a cyclindrical symmetry around the Fe-Ω axis, analogous to what one would expect in ferrocene. This is best seen in Figure 5 (right). The

Table VII. Bond Lengths (Å) and Angles (deg)

	X ray (full set)	Neutron data	Neutron (corrected for thermal librations)
Fe-Fe′	2.5389 (3)	2.5390 (6)	2.541
Fe-C(1)	1.7611 (8)	1.7626 (6)	1.765
Fe-C(2)	1.9279 (8)	1.9280 (5)	1.931
Fe-C(2)′	1.9204 (8)	1.9210 (6)	1.923
Fe-C(11)	2.1377 (8)	2.1392 (6)	2.142
Fe-C(12)	2.1355 (9)	2.1360 (6)	2.139
Fe-C(13)	2.1014 (8)	2.1036 (6)	2.105
Fe-C(14)	2.1168 (8)	2.1173 (6)	2.119
Fe-C(15)	2.1447 (8)	2.1456 (6)	2.148
Fe-Ω	1.7511	1.7512	1.753
C(1)-O(1)	1.1505 (10)	1.1498 (8)	1.152
C(2)-O(2)	1.1799 (9)	1.1782 (7)	1.180
C(11)-C(12)	1.4200 (13)	1.4231 (8)	1.429
C(12)-C(13)	1.4145 (13)	1.4165 (8)	1.422
C(13)-C(14)	1.4327 (13)	1.4351 (8)	1.441
C(14)-C(15)	1.4128 (12)	1.4106 (8)	1.416
C(15)-C(11)	1.4203 (12)	1.4249 (8)	1.431
C(11)-H(11)	0.974 (14)	1.0802 (13)	1.107
C(12)-H(12)	0.952 (15)	1.0779 (14)	1.106
C(13)-H(13)	0.975 (14)	1.0787 (13)	1.105
C(14)-H(14)	0.996 (13)	1.0791 (13)	1.105
C(15)-H(15)	0.987 (15)	1.0820 (13)	1.107
C(2)-Fe-C(2)′	97.44 (3)	97.45 (2)	
C(1)-Fe-C(2)	93.01 (4)	92.95 (3)	
C(1)-Fe-C(2)′	94.54 (4)	94.61 (3)	
C(1)-Fe-Fe′	95.72 (3)	95.73 (2)	
Fe-C(1)-O(1)	178.48 (8)	178.43 (5)	
Fe-C(2)-O(2)	137.99 (6)	137.96 (5)	
Fe-C(2)-Fe′	82.56 (3)	82.55 (2)	
C(15)-C(11)-C(12)	108.19 (7)	108.01 (5)	
C(11)-C(12)-C(13)	107.76 (8)	107.78 (5)	
C(12)-C(13)-C(14)	108.23 (8)	108.20 (5)	
C(13)-C(14)-C(15)	107.52 (7)	107.61 (5)	
C(14)-C(15)-C(11)	108.28 (7)	108.38 (4)	
H(11)-C(11)-C(12)	125.0 (8)	125.66 (9)	
H(12)-C(12)-C(13)	127.1 (8)	126.08 (10)	
H(13)-C(13)-C(14)	125.7 (8)	126.02 (9)	
H(14)-C(14)-C(15)	127.8 (8)	127.07 (9)	
H(15)-C(15)-C(11)	125.9 (7)	125.76 (10)	

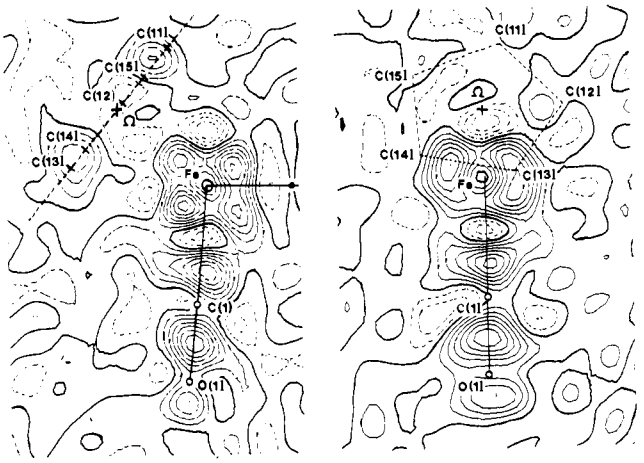

Figure 3. Section of the deformation density by two perpendicular planes containing the terminal carbonyl C(1) O(1). Contour interval: 0.1 e Å^{-3}. Dashed contours for negative, bold line for zero deformation density. Resolution: 2 sin θ_{max}/λ = 1.52 Å^{-1}.

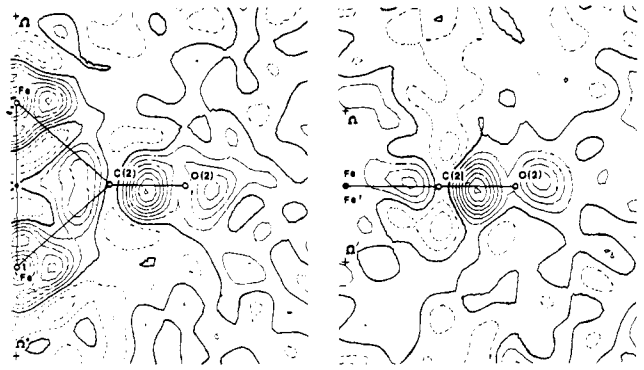

Figure 4. Section of the deformation density by two perpendicular planes containing the bridged carbonyl C(2) O(2). Contours and resolution as in Figure 3.

iron nucleus, at which position the deformation density is practically zero, is surrounded by a ring of an almost uniform deformation density of about 0.5 e Å^{-3}, parallel to the cyclopentadienyl plane.

To gain some insight into the bonding in bis(dicarbonyl-π-cyclopentadienyliron), a simple semiempirical molecular orbital calculation has been performed. The method used was SCCCMO,[20] an iterative calculation of the extended-Hückel

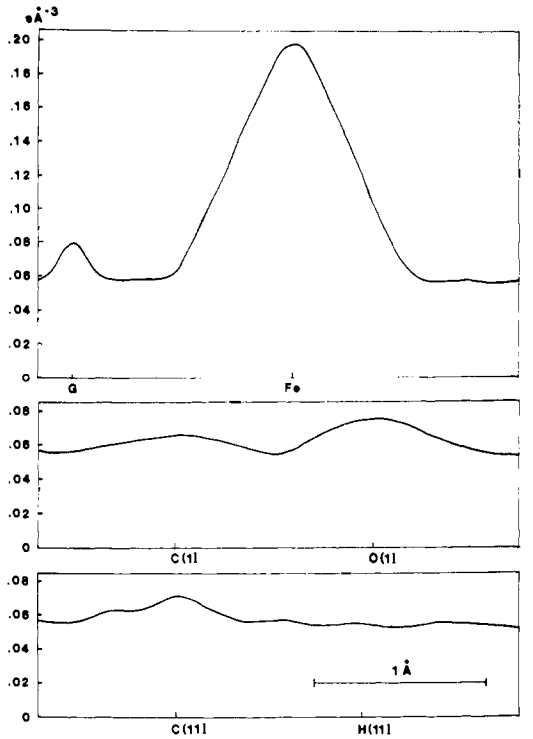

Figure 6. Estimated standard deviation of the deformation density $\sigma(\Delta\rho)$ along three bond axes. $\sigma(\rho_{obsd})$ is 0.055 e Å^{-3} in average at a general position, 0.078 e Å^{-3} at the crystallographic inversion center G.

type. The basis consisted of the 3d, 4s, and 4p orbitals of the iron atoms, the 1π, 5σ, and 2π (or π*) orbitals of the carbonyls, and the five π orbitals of cyclopentadienyl. The geometry was idealized by assuming a mirror plane for the whole molecule and a fivefold symmetry of the cyclopentadienyl ring. The z axis was taken perpendicular to the cyclopentadienyl ring, the y axis perpendicular to the molecular mirror plane. Some results of the Mulliken population analysis are reported in Table VIII.

The small negative overlap population between the two iron atoms may be related to the lack of significant features in the deformation density maps. When the z axis is chosen along the Fe–Fe direction, a positive Mulliken overlap population is found only between the $3d_{z^2}$ orbitals (+0.03 electron), indicating a very weak σ bond. Examination of the molecular orbital coefficients shows that one of the highest occupied MOs is antibonding with respect to the d_{z^2} orbitals, in contrast to

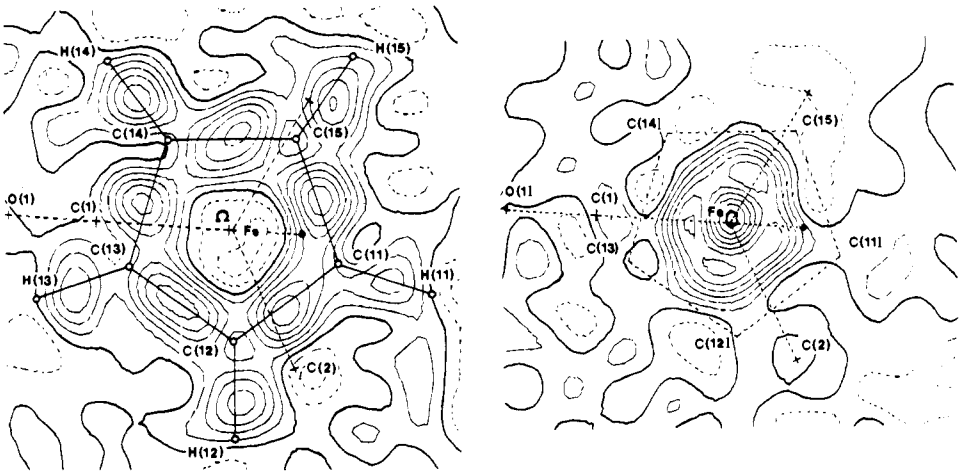

Figure 5. Section of the deformation density in the cyclopentadienyl plane (left) and a parallel plane through the iron nucleus (right). Contours and resolution as in Figure 3.

Table VIII. Mulliken Electron Populations from SCCCMO Calculation

Orbital populations			
Fe 3 d_{z^2}	1.86	C_5H_5 e_1^+	1.77
$d_{x^2-y^2}$	1.67	e_1^-	1.64
d_{xy}	1.67	C(1) O(1) 5σ	1.65
d_{yz}	1.38	π^*	0.26
d_{xz}	0.86	C(2) O(2) 5σ	1.56
4 s	0.21	π^*	0.39
p_x	0.03		
p_y	0.06		
p_z	−0.01		
Metal and ligand charges			
Fe	+0.28		
C_5H_5	−0.40		
C(1) O(1)	+0.11		
C(2) O(2)	+0.01		
Overlap populations			
Fe-Fe	−0.14	C(1)-O(1)	0.55
Fe-C_5H_5	0.43	C(2)-O(2)	0.45
(d_{yz}-e_1^+	0.05	C(11)-C(12)	0.21
d_{xz}-e_1^-	0.15)	C(12)-C(13)	0.23
Fe-C(1)O(1)	0.42	C(13)-C(14)	0.18
Fe-C(2)O(2)	0.30		

$Mn_2(CO)_{10}$,[21] and to the complexes $Fe_2(CO)_6X_2$ (X = S, SCH_3, NH_2, NCH_3),[22] where the highest occupied molecular orbital (HOMO) was found to be a bonding combination of the d_{z^2} orbitals, whereas the lowest unoccupied MO (LUMO) was the antibonding counterpart. The metal-metal bond would thus be weaker in our carbonyl-bridged complex than in $Mn_2(CO)_{10}$ or in $Fe_2(CO)_6X_2$. This is, however, contradicted by the bond dissociation energies, which are of the same order of magnitude in $[C_5H_5Fe(CO)_2]_2$ and in $Mn_2(CO)_{10}$.[23]

There is no doubt that the two iron atoms are linked by a true chemical bond. This is further evidence by the diamagnetic behavior of the complex, which implies spin coupling, and also by the short iron-iron distance (2.541 Å vs. 2.482 Å in metallic iron). Rather than the existence of the bond, what must be called in question is the intuitive concept that bonding implies necessarily a concentration of electron density between the bonded atoms. Such a concentration is indeed observed between first-row atoms, but the overlap between the 2p orbitals is an order of magnitude larger than the overlap of the 3d orbitals in a metal-metal complex. This small overlap could provide a qualitative explanation for the observed deformation density. A shorter metal-metal separation would enable a better overlap, but at the cost of a larger repulsion between the electron cores. On the other hand, the overlap of the 4p orbitals is much better, but their energy is too high for their use in the bonding.

Compared to free carbon monoxide, the configuration of the bridged carbonyl C(2) O(2) is more deeply altered than that of the terminal carbonyl C(1) O(1), which is not unexpected, as the former is bonded to two iron atoms, with an overlap population in each bond only slightly smaller than that of Fe-C(1)O(1) (0.30 compared to 0.42 electron). The formal electron transfers between the metal and CO, for direct and back-bonding, are 0.35 and 0.25 electron, respectively, for the terminal carbonyl and 0.44 and 0.49 electron for the bridged carbonyl. These differences in the electron configuration agree with the experimental C-O bond lengths (terminal carbonyl, 1.152 Å; bridged carbonyl, 1.180 Å). From the calculated difference of 0.1 electron in the occupancy of the 5σ orbitals, one would expect the carbon lone-pair peak of the terminal carbonyl to be higher than that of the bridged carbonyl by an amount of 0.1-0.2 e $Å^{-3}$ (the dynamic electron density for one electron in the 5σ orbital peaks at about 1.5 e $Å^{-3}$ in the carbon lone-pair region[19]). Such an effect is indeed observed, though larger than expected (0.3 e $Å^{-3}$). On the other hand, no significant difference is seen in the $p\pi$ regions between the two carbonyl groups, in spite of the different occupancy of the π^* orbitals.

Other results of the MO calculation can be rationalized as follows. The orbitals of cyclopentadienyl which are implied in bonding are essentially e_1^+ and e_1^- which are doubly degenerate in a symmetric field. e_1^+ is antisymmetric relative to the mirror plane of the molecule, and overlaps with the metal orbital $3d_{yz}$; e_1^- is symmetric and overlaps with $3d_{xz}$ (see, e.g., ref 24). Since there are two iron atoms in the molecule, there are two bonding and two antibonding combinations for each orbital pair e_1^+-d_{yz} and e_1^--d_{xz}. The highest occupied MO is essentially the lowest antibonding combination e_1^+-d_{yz}. Some bonding character between $3d_{xy}$ and the π^* orbitals of C(2) O(2) stabilizes this orbital compared to the similar antibonding combination e_1^--d_{xz}, which forms the lowest unoccupied MO. The consequences are seen in the table: (a) a larger occupancy of d_{yz} than of d_{xz} (both orbitals, however, are less occupied than d_{z^2}, $d_{x^2-y^2}$, and d_{xy}, which are less engaged in bonding); (b) a larger occupancy of e_1^+ than of e_1^-; (c) an overlap population d_{yz}—e_1^+ smaller than d_{xz}-e_1^-. The different occupancy of e_1^+ and e_1^- is responsible for the different overlap populations of the C-C bonds, the sequence of which is in quite good agreement with our experimental bond lengths (Figure 2). The possible occurrence of distortions in the cyclopentadienyl rings has been abundantly discussed a few years ago.[24,25] An "allyl-ene" type structure, in which the e_1^- orbital is predominant, is sometimes invoked.[26-28] However, owing principally to the large anisotropic thermal motion of the ring in most complexes at room temperature, the precision of the experimental results is rarely sufficient to establish the existence of such a distortion. This is the first example, to our knowledge, where significant distortions of the cyclopentadienyl ring indicate the predominance of the e_1^+ orbital.

The asphericity of electron density around the nuclei is seen at best in a section of the deformation density by a sphere of suitable radius centered on the metal nucleus. The stereographic projection of such a spherical section is shown in Figure 7 (left). A radius of 0.65 Å was chosen. This is approximately the distance at which the largest asphericity effects are observed, as expected theoretically if they are due to unequal occupanices of the 3d orbitals.[19] Figure 7 (left) is the average of the two hemispheres separated by the molecular "mirror" plane, which were very similar. The approximate local centrosymmetry around the metal nucleus, seen in the planar and spherical sections, is an indication that the asphericity in the metal region is due essentially to the 3d electrons: if the 4p orbitals were playing an important role, the mixing of odd p functions with even d functions in the same MOs would result in noncentrosymmetric features. This is in agreement with the small populations of the 4p orbitals in the SCCC calculation (Table VIII).

It is possible to calculate a theoretical asphericity, as the function

$$\Delta\rho_{calcd}(r,\theta,\phi) = \sum_k \sum_l D_{kl}(3d)_k(3d)_l - \sum_k D_{kk}R(r)^2/(4\pi)$$

$$= R(r)^2\left[\sum_k \sum_l D_{kl}Y_k(\theta,\phi)Y_l(\theta,\phi) - \sum_k D_{kk}/(4\pi)\right]$$

where $(3d)_k$ is the atomic orbital $(3d)_k = R(r)Y_k(\theta,\phi)$ and **D** is the density matrix related to the coefficients C_{ki} of the doubly occupied molecular orbitals: $D_{kl} = \Sigma_i 2C_{ki}C_{li}$. The second term of $\Delta\rho_{calcd}$ is the average of the first term over the whole sphere of radius r, so that the integral of $\Delta\rho_{calcd}$ over the whole sphere is zero. It should be emphasized that $\Delta\rho_{calcd}/R(r)^2$ depends only on the relative occupancy of the 3d orbitals and not on the exact value assumed for these orbitals. The radial part $R(r)$ may be considered as a simple scale factor. A qualitative comparison with the observed deformation

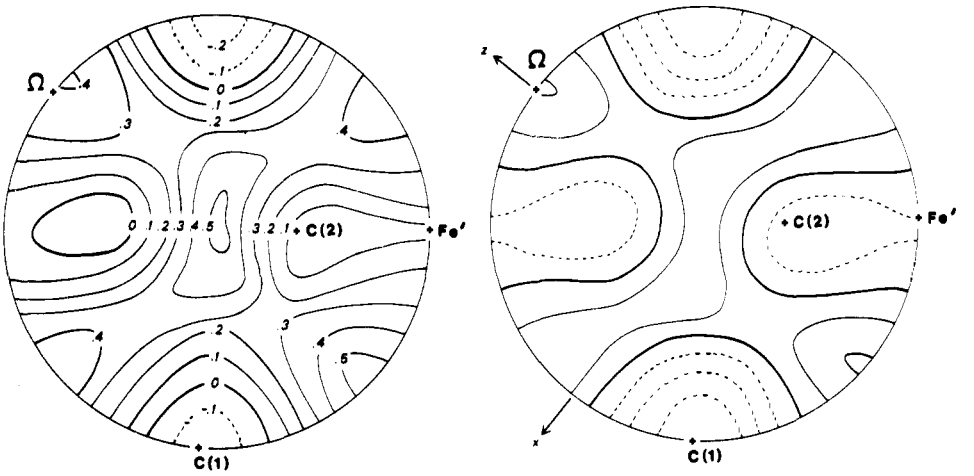

Figure 7. Left: section of the deformation density by a sphere of radius 0.65 Å, centered on Fe (stereographic projection, average between the two hemispheres). An atom designation A represents the direction Fe-A. Ω is the direction of the center of the cyclopentadienyl ring. Unit: e Å^{-3}. Right: asphericity due to unequal occupancy of the Fe 3d orbitals, from a SCCCMO calculation. Units: $R(r)^2/4\pi$. The axes chosen for the MO calculation are shown.

density seems therefore not unreasonable, provided that (a) the other iron orbitals do not contribute strongly to the asphericity; (b) the radius r is small enough so that the contribution from orbitals centered on different atoms may be neglected. A comparison of this kind is quite different from a general comparison of observed and calculated difference density, which, owing to the large number of parameters involved and to the drastic approximations of the calculation, would be of questionable significance.

Figure 7 (right) is a plot of $\Delta\rho_{\text{calcd}}$. The qualitative agreement between the experimental and the theoretical map is rather good, and indicates that the relative occupancy of the five 3d orbitals is satisfactorily reproduced by the SCCC calculation. The two maps show a concentration of electron density in the direction of the center Ω of the cyclopentadienyl ring, and in the plane parallel to the ring, which, with our choice of axes, are the regions of the d_{z^2}, $d_{x^2-y^2}$, and d_{xy} orbitals. Minima are seen in both maps in the direction of the carbon atoms of the carbonyls (and in the opposite directions), deeper in the direction of the terminal carbonyl C(1) that in that of the bridged carbonyl C(2).

An ab initio calculation on this complex, presently performed by M. Benard and A. Veillard, should enable a more quantitative comparison with our experimental results.

Acknowledgments. We are grateful to the Institut Max von Laue-Paul Langevin, for providing experimental facilities, technical assistance, and financial support to one of us (A.M.) during the neutron measurements. We thank Dr. A. Veillard and M. Benard for their interest in our results and for useful discussions.

Supplementary Material Available: A list of observed and calculated structure factors (33 pages). Ordering information is given on any current masthead page.

References and Notes

(1) (a) Université Louis Pasteur; (b) Institut Max von Laue-Paul Langevin.
(2) (a) W. E. Hatfield and J. S. Paschal, *J. Am. Chem. Soc.*, **86**, 3888–3889 (1964); (b) J. M. Coleman and L. F. Dahl, *ibid.*, **89**, 542–552 (1967).
(3) O. S. Mills, *Acta Crystallogr.*, **11**, 620–623 (1958).
(4) R. F. Bryan and P. T. Greene, *J. Chem. Soc. A*, 3064–3068 (1970).
(5) R. F. Bryan, P. T. Greene, M. J. Newlands, and D. S. Field, *J. Chem. Soc. A*, 3068–3073 (1970).
(6) P. Coppens, F. K. Ross, R. M. Blessing, W. F. Cooper, F. K. Larsen, J. G. Leipoldt, B. Rees, and R. Leonard, *J. Appl. Crystallogr.*, 7, 315–319 (1974).
(7) M. S. Lehmann, S. A. Mason, and P. Simms, to be published.
(8) M. S. Lehmann and F. K. Larsen, *Acta Crystallogr., Sect. A*, 580–584 (1974).
(9) "International Tables for X-Ray Crystallography", Vol. IV, Kynoch Press, Birmingham, England, 1974.
(10) P. J. Becker and P. Coppens, *Acta Crystallogr., Sect. A*, **30**, 129–147, 148–153 (1974); **31**, 417–425 (1975).
(11) M. Sakata and J. Harada, *Acta Crystallogr., Sect. A*, **32**, 426–433 (1976).
(12) R. B. Helmholdt and A. Vos, *Acta Crystallogr., Sect. A*, **33**, 38–45 (1977).
(13) V. Schomaker and K. N. Trueblood, *Acta Crystallogr., Sect. B*, **24**, 63–76 (1968).
(14) R. K. Bohn and A. Haaland, *J. Organomet. Chem.*, **5**, 470–476 (1966).
(15) B. Rees and P. Coppens, *Acta Crystallogr., Sect. B*, **29**, 2516–2528 (1973).
(16) F. A. Cotton and J. M. Troup, *J. Chem. Soc., Dalton Trans.*, 800–802 (1974).
(17) B. Rees, *Acta Crystallogr., Sect. A*, **34**, 254–256 (1978).
(18) Y. Wang and P. Coppens, *Inorg. Chem.*, **15**, 1122–1127 (1976).
(19) B. Rees and A. Mitschler, *J. Am. Chem. Soc.*, **98**, 7918–7924 (1976).
(20) D. A. Brown and R. M. Rawlinson, *J. Chem. Soc. A*, 1534–1537 (1969).
(21) R. A. Levenson and H. B. Gray, *J. Am. Chem. Soc.*, **97**, 6042–6047 (1975).
(22) B. K. Teo, M. B. Hall, R. F. Fenske, and L. F. Dahl, *Inorg. Chem.*, **14**, 3103–3117 (1975).
(23) A. R. Cutler and M. Rosenblum, *J. Organomet. Chem.*, **120**, 87–96 (1976).
(24) M. J. Bennett, M. R. Churchill, M. Gerloch, and R. Mason, *Nature (London)*, **201**, 1318–1320 (1964).
(25) P. J. Wheatley in "Perspectives in Structural Chemistry", Vol. I, J. D. Dunitz and J. A. Ibers, Ed., Wiley, New York, N.Y., 1967, pp 1–40.
(26) M. Gerloch and R. Mason, *J. Chem. Soc.*, 296–304 (1965).
(27) M. R. Churchill, *Inorg. Chem.*, **4**, 1734–1739 (1965).
(28) A. E. Smith, *Inorg. Chem.*, **11**, 165–170 (1972).